Melanoregulin Deficiency Affects Bone Maintenance and Lean Body Mass

M.L. Musskopf[1ǂ], V. De P. Gonçalves[2ǂ], S. Tuin[3], S.W. Wong[4], K. Boesze-Battaglia[5], P.A. Miguez[4,*]

[1]Department of Restorative Sciences, Adams School of Dentistry, UNC-CH, Chapel Hill, NC, USA

[2]Department of Dentistry, Pontifical Catholic University of Minas Gerais, Belo Horizonte, Brazil

[3]Adams School of Dentistry, UNC-CH, NC, USA

[4]Department of Periodontology, Endodontics and Dental Hygiene, Adams School of Dentistry, UNC-CH, Chapel Hill, NC, USA

[5]Department of Basic & Translational Sciences, University of Pennsylvania School of Dental Medicine, Philadelphia, PA, USA

*Corresponding author:

Patricia A. Miguez, DDS, MS, PhD
Associate Professor
Department of Periodontology, Endodontics and Dental Hygiene
Adams School of Dentistry
University of North Carolina at Chapel Hill
CB#7450
miguezp@unc.edu

ǂThese authors contributed similarly to the work.

ABSTRACT

Objectives: Studies documented the association of melanoregulin (MREG), a cargo-sorting protein, with its binding partner, the autophagic protein, microtubule-associated protein 1 light chain 3B (LC3B) in macrophages which could affect bone physiology due to the importance of autophagy in osteoclast function. Herein we propose to test the hypothesis that MREG modulates bone remodeling. Therefore, we analyzed the *Mreg*$^{dsu/dsu}$ mutant mice for bone mass, growth plate microarchitecture, and bone marrow-derived osteoclast function to understand how lack of MREG affects bone and mass at two different time points.

Methods: Mice femurs from wild type and MREG$^{-/-}$ male mice (on C57BL6)/J background) were harvested at 4 and 10 months and imaged by microcomputed tomography to assess bone mass parameters. Femurs were processed for histology by H&E and TRAP staining for assessment of osteoclast numbers. Primary bone marrow-derived macrophages from 3-week-old mice were harvested to assess osteoclast differentiation and function via TRAP, resorptive assay and Western Blot for osteoclast differentiation markers. In addition, a separate cohort of mice were analyzed via EchoMRI to characterize total lean vs. fat whole body mass.

Results: There was a statistically significant difference in bone volume of 10-month old mice in wild type vs. MREG$^{-/-}$ with MREG mutation suggesting a preservative effect on phenotypical bone parameters as the mice age. A reduction in adipose tissue but an increase in osteoclast numbers was found histologically in MREG mutant femurs. Bone marrow-derived cells, however, showed reduced osteoclastic function in MREG$^{-/-}$. The mutant mice presented a total lean mass significantly increased compared to wild type per EchoMRI.

Conclusions: MREG deficiency seems to impact osteoclast numbers *in vivo* but not *in vitro*, although *in vitro* function was reduced. MREG deficiency favors lean mass preservation over fat accumulation in bones and body composition as mice age. This study provides the foundation for a more in-depth investigation of MREG's role in bone and systemic metabolism. It is possible that MREG can be a future target for new therapeutic modalities in inflammatory and metabolic bone diseases.

KEYWORDS: Bone, autophagy, osteoclast, melanoregulin, fat metabolism

INTRODUCTION

Bone is a metabolically active tissue with a network structure constituted of different types of cells and regulated by various biological, biochemical and physical factors. The maintenance of a stable bone metabolism requires the continuous differentiation and maturation of different progenitor cells, the preservation of the mineralizing function of osteoblasts, the resorptive capacity of osteoclasts, the secretion of factors that regulate interactions between cells and the extracellular matrix (1-5). Bone remodeling is essential for the formation and maintenance of bone morphology and the regeneration of damaged bone (6, 7), and a dysfunction of any cell type involved in this process can lead to the failure of these preocesses followed by the development of conditions such as osteoporosis (7, 8).

Autophagy plays an important role in maintaining cellular function and it is a complex dynamic process involved in the degradation of intracellular proteins and organelles under different physiological or pathological conditions(1). It is a vital function to maintain cell homeostasis in response to starvation, hypoxia, infection, and other stressful stimuli (1, 3, 7, 9). In bone tissue, autophagy plays key functions in bone marrow mesenchymal stem cells (BMSCs) and derived cells including chondrocytes, osteoblasts and osteocytes (3, 10).

Osteoblasts are specialized mesenchymal-derived cells involved in bone formation, and impaired autophagy in these cells has been shown to lead to decreased bone mass, while inhibiting autophagy in osteocytes results in bone tissue senescence (11-13). Previous evidence showed that altered autophagy inhibits the function of endogenous BMSCs and further promotes the development of osteoporosis (14, 15). *In vitro* studies demonstrated that downregulation/ablation of autophagy markers resulted in the dysfunction or inhibition of osteoblast differentiation (11, 16, 17). Complementary, *in vivo* studies have showed that knockout of autophagy-related genes in mice, resulted in impaired mineralization and reduced bone mass (16, 18).

Moreover, it has been shown that undifferentiated mesenchymal stem cell (MSCs) contain more autophagosomes than differentiated ones, suggesting that autophagy is correlated with MSC differentiation (3). When those cells are exposed to osteogenic stimulation, the accumulated autophagosomes can degrade rapidly, providing the corresponding energy and metabolic precursors for the morphological, function, and metabolic changes required for cell differentiation (19). In corroboration, it is known that during early-stage osteogenic differentiation, the expression of autophagosome marker LC3-II is reduced within 12h, suggesting that these accumulated autophagic vacuoles may serve as a source of rapidly produced energy substrates to support differentiation (20, 21). Frost et al. reported how *P. Gingivalis'* lipopolysaccharide (LPS)1690 affects autophagy

assessing LC3-dependent and MREG-dependent processes in green fluorescent protein -LC3-expressing Saos-2 cells (pre-osteoblastic cells) (22). The authors observed that LPS stimulated the formation of very large LC3-positive vacuoles and MREG puncta, as they work together in autophagosome formation.

Further, autophagic proteins are also necessary for osteoclast-directed bone resorption (23, 24) and previous studies have reported that increased authopagy in osteoclasts stimulated cell differentiation and osteoclastogenesis leading to increased bone resorption. I*n vitro* the knockdown of autophagy-related genes in osteoclasts has been shown to significantly reduce the depth and volume of bone resorptive pits (24-28). To further elucidate the role of MREG in bone, we investigated the phenotype of MREG-deficient mice in skeletal bone. Given MREG's documented role in endolysosomal trafficking and LC3-dependent processes in other cell types, and its expression in bone tissue, investigating its function in bone remodeling is warranted (21, 22). We hypothesize that since MREG is involved in the autophagy process, its deficiency may be implicated in bone physiology and will lead to positive associated bone changes (bone preservation) with maturation of bones. The purpose of this study was to characterize the femoral bone phenotype of the MREG knockout mice and acquire further insight into MREG function not only in osteoclast cell differentiation and function but also evaluate the resulting bone phenotype in the context of development and maturation.

MATERIAL AND METHODS

Animals

Melanoregulin (MREG) is the product of the $Mreg^{dsu}$ gene locus [previously known as dilute suppressor (*dsu*) (29). $Mreg^{dsu/dsu}$ mice carry the $Mreg^{dsu}$ allele (mouse accession number Q6NV65), in which the deletion of the first two exons results in an effective null allele. $Mreg^{dsu/dsu}$ mice (on C57BL6/J genetic background) used in these studies were originally maintained and propagated at the NCI, National Institutes of Health, [generous gifts from Drs. N. Jenkins and N. Copeland (Texas Medical Center)]. Both $Mreg^{dsu/dsu}$ and $MREG^{+/+}$ [C57Bl6/J mice, (obtained from the Jackson Laboratory)] mice were housed under standard cyclic light conditions: 12-h light/12-h dark and fed ad libitum.

The animal experiment protocol was approved by the Institutional Animal Care and Use Committee (IACUC) at the University of North Carolina at Chapel Hill (IACUC ID: 22-053). The procedures were also conducted in compliance with ethical standards that fully comply with Animal Research:

Reporting of *In Vivo* Experiments (ARRIVE) guidelines. Male MREG$^{+/+}$ and MREG$^{-/-}$ mice (on C57BL6)/J genetic background) at 6 weeks of age (20–27 g) were kept in an environment with controlled temperature, humidity, and light cycles, and fed with water and feed ad libitum. Mice were aged up to 10 months. Briefly, mice femurs were harvested at 4 and 10 months and imaged by microcomputed tomography to assess bone mass parameters, femurs processed for histology and stained by hematoxylin and eosin (H&E) for structural and tartrate resistant acid phosphatase (TRAP) for osteoclast numbers assessment. Mice were also scanned via magnetic ressonance to characterize total lean vs. fat mass. Primary bone marrow-derived macrophages from 3-week-old mice were harvested to assess osteoclast function as described below.

Microcomputed Tomography

After mice reached 4 and 10 months of age, animals were sacrificed under humane conditions as approved by IACUC. Femurs and heads were harvested from 4-5 mice from each group, fixed in 10% buffered formalin for 3 days under constant agitation and stored in PBS at 4°C until dissected for imaging. Sample size was determined from previous studies showing similar bone volume effects (30). The femurs were scanned using a microcomputed tomography (µCT) system (Skyscan 1275, Bruker) at 12.45 µm, 70 kVp, 142 µA using a 0.5 mm aluminum attenuation filter. The three-dimensional images were reconstructed using the software NRecon 1.6.9.8 (SkyScan), Data Viewer 1.5.0 (SkyScan) and CTAnalyzer (CTAn—2003-11SkyScan, 2012 Bruker MicroCT, 1.13.11.0 version) and were used for image re-orientation and analysis, respectively. For the analysis, a standardized region of interest (ROI) included a set of specific number of slices below the growth plate after a set anatomical marker for trabecular bone and cortical bone analysis (50 and 400 slices below growth plate, respectively). The bone microarchitecture parameters evaluated were trabecular and cortical bone volume fraction (BV/TV, %), trabecular thickness (Tb.Th), trabecular number (Tb.N), trabecular separation (Tb.S), as the recommended parameters reported by Bouxsein et al. and as we previously reported (30, 31).

Histological analysis

After the femurs were demineralized in EDTA ph 7.4 for 4 weeks, they were embedded, non-serial histological sections (6 µm) were obtained and stained by H&E for a qualitative gross evaluation.

For TRAP staining, slides were deparaffinized and rehydrated through graded ethanol to distilled water, and then immersed in TRAP staining solution mix (at 37°C for 30 minutes). The sections were rinsed in distilled water and counterstained with 0.02% fast green for 30 seconds. For quantification, TRAP-positive cells stained in red and containing three or more nuclei on the bone surface, were considered osteoclasts, and quantified in the region of interest immediately below the growth plate as we previously reported (24).

WT and MREG$^{-/-}$ primary osteoclasts harvest, differentiation and function

In a separate cohort of animals, after euthanasia by CO2, tibias and femurs were harvested from 3 week-old MREG$^{+/+}$ /MREG$^{-/-}$ mice (on C57BL6)/J genetic background). Three independent experiments were performed, each using bone marrow pooled from 3 mice per genotype with triplicates. Bone marrow cells were flushed into the phenol-free α-MEM medium, supplemented with 10% FBS, L-glutamine, nonessential amino acids, and penicillin/streptomycin. Non-adherent cells were harvested after 24 h and re-plated at a density of $1.5x10^5$ cells/cm2 with 30 ng/mL M-CSF (R&D Systems, Minneapolis, MN, USA). After 2 days, the medium was replenished with 30 ng/mL M-CSF and 10 ng/mL RANKL (R&D Systems Minneapolis, MN, USA) for osteoclast differentiation. After 5 days of culture, cells were fixed and stained with TRAP. Equal numbers of bone marrow osteoclast precursors were plated and differentiated on Osteo Assay Surface plates (Corning Lifesciences, Tewksburg, MA, USA) for resorption assay. At day 5, the plate was bleached, and areas of resorption pits were quantified using NIH ImageJ (24, 32).

Bone marrow osteoclast precursors were plated and differentiated by 3 days for Western Blot (WB) analysis. On days 0, 1, and 2 of the assay, the supernatant of each well plate was aspirated and cells harvested. Briefly, RIPA Buffer solution (ThermoFisher Scientific, Waltham, MA, USA) containing protease inhibitors was added into the plates and using a scraper, the cells were detached and transferred to Eppendorf tubes and kept at −80 °C. Protein quantification was performed using the BCA Protein Kit (Pierce BCA Protein Kit, Thermo Fisher Scientific, Waltham, MA, USA) according to the manufacturer's guidelines and samples were prepared WB to evaluate the protein expression of c-Fos (Cat. #4384s, Cell Signaling, Danvers, MA, USA), NFATc1 (Cat. #sc-7294, Santa Cruz Biotechnology, Dallas, TX, USA) and as a control, β-actin 1 (Cat. #sc-1616, Santa Cruz Biotechnology). In total, 5-10 µg of the total protein lysate was resolved using Criterion TGX precast gel (Biorad, Hercules, CA, USA) and transferred to a nitrocellulose membrane using the Trans-Blot Turbo Transfer System (Biorad) and immunodetected using appropriate primary and peroxidase-

coupled secondary antibodies (Goat-Anti-Rabbit IgG, ThermoFisher #31460). Proteins were visualized using enhanced chemiluminescence (ECL, Amersham Bioscience, Chicago, IL, USA). The protein levels were evaluated relative to β-actin via use of Image J (NIH, Bethesda, MD, USA) (24).

Echo MRI

Metabolic studies including echo-magnetic resonance imaging (EchoMRI) experiments were conducted as previously described (33). Briefly, 7 live mice, WT and MREG mutants, at 10 months of age, were placed in a specially sized, clear plastic holder without sedation or anesthesia. The tube is 2-inches in diameter with 2-5 inches adjustable length and can fit mice up to 100g in weight. There was a total of eight quarter-inch diameter air holes on each side of the tube to ensure air exchange. The tube (with a mouse inside) was then inserted into the tubular space of the EchoMRI™ system. The scans took place for 2 minutes. The fat/lean mass and body water measurements were recorded in grams. No pain or any physical damage was incurred during the measurements.

Statistical analyses

For all *in vitro* data, three independent experiments were performed, and each experiment was conducted in triplicate sets. Statistical analysis treated the experiment of cells harvested from mice as the unit of analysis (n=3). For μCT, n=5 for WT, n=4 MREG$^{-/-}$ at 4 months; n=5 per group at 10 months. For Echo MRI, the n=7. Histological quantification of osteoclasts: n=4 per group with 3 sections per animal. For both, *in vitro* and *in vivo* assays, data were submitted to the Kolmogorov–Smirnov or Shapiro–Wilk tests to assess homogeneity and data distribution. Student's *T* test or analysis of variance (ANOVA) were used to determine the differences among groups. All analyses were performed using GraphPad Prism 8 software (GraphPad Software Inc., San Diego, CA, USA). All tests were applied with a 95% confidence level ($p < 0.05$). Data were expressed as mean ± standard deviation.

RESULTS

MREG deletion promoted an age-dependent bone-sparing effect on femoral bone

Trabecular structure using µCT showed that there was no difference in trabecular separation (Tr.Sp), number (Tr.N) and thickness (Tr.Th) between MREG$^{-/-}$ and WT mice at 4 months [Figure (fig) 1A, B]. At 10 months, bone parameters were significantly improved for MREG mutants such as Tr.N and bone volume variables ($p < 0.05$). (Fig. 1C, D). Cortical parameters were not statistically different between age groups (Fig. 1E).

MREG$^{-/-}$ femurs showed increased osteoclast numbers and decreased evidence of adipocyte population

Qualitative histological assessment of the femurs for gross differences in bone morphometry revealed that marrow-associated adipose tissue was markedly different between MREG$^{-/-}$ and WT. The adipose cells just below the growth plate area was absent in MREG$^{-/-}$ (Fig. 2A, B). Quantititative analysis of osteclasts by TRAP+ multinucleated cell numbers was similar for 4-month-old WT mice (Fig. 3A, B) and MREG$^{-/-}$ ($p > 0.05$). However, in 10-month-old MREG$^{-/-}$ mice there was an increase in osteoclast count (Fig. 3C, D, E) ($p < 0.05$) showing that MREG mutation affected the numbers of osteoclasts as the mice aged.

MREG$^{-/-}$ bone marrow cells differentiation and function ex vivo

Primary bone marrow cells harvested from MREG$^{-/-}$ and WT showed similar osteoclast differentiation over time (Fig. 4A). Immunoblotting did not show any difference for master osteoclast differentiation markers, such as NFATC1 and c-Fos (Fig. 4B). However, the resorption pit activity was significantly reduced in MREG mutant osteoclasts (Fig. 4C,D) ($p < 0.05$).

MREG$^{-/-}$ mice showed higher total body lean mass

EchoMRI was used to assess the ratio of lean to adipose mass as reported (33). We observed a statistical difference between MREG$^{-/-}$ and WT mice. The fat/bone ratio decreased for MREG$^{-/-}$ at 10 months (Fig. 5A, B) ($p < 0.05$). The lean mass number was statistically higher for older MREG$^{-/-,}$ although they did not differ in weight (Fig. 5A).

DISCUSSION

This study aimed to evaluate bone phenotypic changes and primary osteoclast effects of melanoregulin deficiency. Through imaging, histological and cell culture methods, this small study suggests an important function of MREG in bone and possibly adipose tissue accumulation. This study shows a contradictory role of MREG deficiency, where it positively affected bone maintenance as observed by computed tomography, but also increased osteoclast numbers as observed histologically. Further, *ex vivo* culture of MREG$^{-/-}$ bone marrow-derived cells shows no difference in cell numbers as they differentiate, but a reduction in their resorptive capacity. The paradoxal observation of increased osteoclast numbers in vivo concurrent with bone-sparing phenotype suggests reduced per-cell resorptive function may exceed the compensatory increase in cell numbers. Potential mechanisms of impaired fusion or altered osteoclast lifespan, upregulation of RANKL or decreased OPG to maintain normal resorption is warranted (26, 34, 35).

It was found that MREG function impairment significantly favors bone density as the mice age while decreasing marrow adipose tissue in the growth plate. Fat accumulation in the marrow is a physiological but undesirable bone phenotype acquired with aging that can lead to frailty and limited regenerative capacity. The phenotype of WT compared to MREG mutants could also be clearly associated with other undesirable metabolic changes such as obesity. This is supported by the finding that the MREG$^{-/-}$ mice are leaner compared to WT, as measured by EchoMRI at 10 months, despite higher bone mass and no statistical difference in weight. The systemic metabolic alterations in MREG$^{-/-}$ mice, including the localized reduced adiposity in bone marrow and increased lean mass is curious but it is important to acknowledge that bone marrow adipose tissue represents less than 1-2% of total body fat (36). Further, MREG deficiency could indirectly affect bone through mechanical loading or hormonal mechanisms independent of direct MREG function in bone cells (37, 38). Further investigation of circulating factors and inflammatory mediators are recommended for these mice besides level of expression of MREG in various types of cells (including osteocytes and osteoblasts), conditional deletion and rescue experiments. In addition, if MREG selectively affects trabecular bone, this site-specific finding will require further investigation.

We have a tentative hypothesis that MREG plays a significant role in cell fate of BMSCs. Since MREG has been shown to be inversely correlated with AKT-mtor signaling, it is possible that its absence will increase mtor and downstream beta-catenin signaling leading to increased osteogenesis and decreased adipogenesis (39-41). Further, autophagy regulation has been associated with metabolic disorders, thus, it is conceivable that MREG disfunction may affect overall systemic metabolism(42). Nonetheless, despite MREG's documented role in autophagy (21, 43), we found no alterations in LC3 in MREG$^{-/-}$ bone cells (not shown) for this cohort of mice, suggesting the

bone phenotype may involve non-canonical autophagy pathways or autophagy-independent MREG functions.

True age-dependent studies to measure skeletal maturity, intermediate points and elderly time points in mice where age-related bone loss is pronounced is also needed to correlate MREG function with bone aging (44). It is a plausible hypothesis that MREG deletion could simultaneously enhance osteoblastogenesis while suppressing adipogenesis and affecting osteoclastogenesis (39, 45).

Our study calls for further definition of which cells are the critical direct target of MREG function in differentiation and explore the mechanism by which the marrow adipose tissue is reduced, and bone density is preserved. Further aging of mice is underway to assess later stages of bone phenotype. After a more thorough characterization of the phenotype of the mice with data on adipose tissue area, fat-related markers, metabolic markers, cell lineage regulation, extensive bone characterization (including sex as a biological variable) and monitoring of autophagy, it will be possible to more holistically assess MREG roles (46, 47). As autophagy regulates cellular energy, as well as aminoacid, glucose and lipid metabolism, the loss of autophagy homeostasis in adipose tissue and other tissues can have drastic effects on local and global metabolism (48, 49).

CONCLUSION

MREG deficiency in male mice seems to affect osteoclast numbers *in vivo* and function and favor lean mass preservation over fat accumulation in bones and body composition as mice mature/age. This study will evolve into a thorough investigation seeking a deeper understanding of MREG and autophagy in bone and systemic metabolism. Understanding MREG function can provide future therapeutic modalities in inflammatory and metabolic diseases possibly related to autophagy.

Acknowledgements and funding

EchoMRI was supported by P30DK056350 awarded to the Nutrition and Obesity Research Center at the University of North Carolina at Chapel Hill. mCT studies were kindly supported by Eric Livingston and Ted Bateman at the School of Biomedical Engineering at UNC-CH. Other mice experiments were supported by UNC Pilot Funds (to P.M.) and NIH R01 DE022465-01A1 (to K.B.B)

Author contribution

M.M: Investigation, Formal Analysis, Validation, Writing- Reviewing and Editing. **V.Dp.:** Investigation, Validation, Writing – First draft. **S.T.:** Investigation, Formal Analysis, Writing – Reviewing and Editing. **S.W.W.:** Investigation, Validation, Writing – Reviewing and Editing. **K.B.:**

Methodology, Resources, Writing – Reviewing and Editing**, P.M.:** Conceptualization, Methodology, Resources, Supervision, Project administration, Visualization, Writing – Original draft, Reviewing and Editing.

REFERENCES

1. Wang S, Deng Z, Ma Y, Jin J, Qi F, Li S, Liu C, Lyu FJ, Zheng Q. The Role of Autophagy and Mitophagy in Bone Metabolic Disorders. Int J Biol Sci. 2020;16(14):2675-91. Epub 2020/08/15. doi: 10.7150/ijbs.46627. PubMed PMID: 32792864; PMCID: PMC7415419.
2. Robling AG, Bonewald LF. The Osteocyte: New Insights. Annu Rev Physiol. 2020;82:485-506. Epub 2020/02/11. doi: 10.1146/annurev-physiol-021119-034332. PubMed PMID: 32040934; PMCID: PMC8274561.
3. Wang J, Zhang Y, Cao J, Wang Y, Anwar N, Zhang Z, Zhang D, Ma Y, Xiao Y, Xiao L, Wang X. The role of autophagy in bone metabolism and clinical significance. Autophagy. 2023;19(9):2409-27. Epub 2023/03/02. doi: 10.1080/15548627.2023.2186112. PubMed PMID: 36858962; PMCID: PMC10392742.
4. Miguez PA. Evidence of biglycan structure-function in bone homeostasis and aging. Connect Tissue Res. 2020;61(1):19-33. Epub 2019/10/11. doi: 10.1080/03008207.2019.1669577. PubMed PMID: 31597498.
5. Miguez PA, Bash E, Musskopf ML, Tuin SA, Rivera-Concepcion A, Chapple ILC, Liu J. Control of tissue homeostasis by the extracellular matrix: Synthetic heparan sulfate as a promising therapeutic for periodontal health and bone regeneration. Periodontol 2000. 2024;94(1):510-31. Epub 2023/08/24. doi: 10.1111/prd.12515. PubMed PMID: 37614159; PMCID: PMC10891305.
6. Martin T, Gooi JH, Sims NA. Molecular mechanisms in coupling of bone formation to resorption. Crit Rev Eukaryot Gene Expr. 2009;19(1):73-88. Epub 2009/02/05. doi: 10.1615/critreveukargeneexpr.v19.i1.40. PubMed PMID: 19191758.
7. Zhu C, Shen S, Zhang S, Huang M, Zhang L, Chen X. Autophagy in Bone Remodeling: A Regulator of Oxidative Stress. Front Endocrinol (Lausanne). 2022;13:898634. Epub 2022/07/19. doi: 10.3389/fendo.2022.898634. PubMed PMID: 35846332; PMCID: PMC9279723.
8. Sućur A, Katavić V, Kelava T, Jajić Z, Kovačić N, Grčević D. Induction of osteoclast progenitors in inflammatory conditions: key to bone destruction in arthritis. Int Orthop. 2014;38(9):1893-903. Epub 2014/06/11. doi: 10.1007/s00264-014-2386-y. PubMed PMID: 24913769.
9. Dikic I, Elazar Z. Mechanism and medical implications of mammalian autophagy. Nat Rev Mol Cell Biol. 2018;19(6):349-64. Epub 2018/04/06. doi: 10.1038/s41580-018-0003-4. PubMed PMID: 29618831.
10. Guan JL, Simon AK, Prescott M, Menendez JA, Liu F, Wang F, Wang C, Wolvetang E, Vazquez-Martin A, Zhang J. Autophagy in stem cells. Autophagy. 2013;9(6):830-49. Epub 2013/03/15. doi: 10.4161/auto.24132. PubMed PMID: 23486312; PMCID: PMC3672294.
11. Li H, Li D, Ma Z, Qian Z, Kang X, Jin X, Li F, Wang X, Chen Q, Sun H, Wu S. Defective autophagy in osteoblasts induces endoplasmic reticulum stress and causes remarkable bone loss. Autophagy. 2018;14(10):1726-41. Epub 2018/07/03. doi: 10.1080/15548627.2018.1483807. PubMed PMID: 29962255; PMCID: PMC6135623.
12. Yin X, Zhou C, Li J, Liu R, Shi B, Yuan Q, Zou S. Autophagy in bone homeostasis and the onset of osteoporosis. Bone Res. 2019;7:28. Epub 2019/11/02. doi: 10.1038/s41413-019-0058-7. PubMed PMID: 31666998; PMCID: PMC6804951.
13. Ma Y, Qi M, An Y, Zhang L, Yang R, Doro DH, Liu W, Jin Y. Autophagy controls mesenchymal stem cell properties and senescence during bone aging. Aging Cell. 2018;17(1). Epub 2017/12/07. doi: 10.1111/acel.12709. PubMed PMID: 29210174; PMCID: PMC5770781.

14. Qi M, Zhang L, Ma Y, Shuai Y, Li L, Luo K, Liu W, Jin Y. Autophagy Maintains the Function of Bone Marrow Mesenchymal Stem Cells to Prevent Estrogen Deficiency-Induced Osteoporosis. Theranostics. 2017;7(18):4498-516. Epub 2017/11/22. doi: 10.7150/thno.17949. PubMed PMID: 29158841; PMCID: PMC5695145.
15. Zhang Y, Li Q, Peng X, Ji P, Zhang Y, Jin J, Yuan Z, Jiang J, Tian G, Cai M, Feng P, Wu Y, Liu W, Wang P. Targeting chaperone-mediated autophagy to regulate osteoclast activity as a therapeutic strategy for osteoporosis. Mater Today Bio. 2025;35:102311. Epub 2025/10/06. doi: 10.1016/j.mtbio.2025.102311. PubMed PMID: 41050091; PMCID: PMC12494939.
16. Liu F, Fang F, Yuan H, Yang D, Chen Y, Williams L, Goldstein SA, Krebsbach PH, Guan JL. Suppression of autophagy by FIP200 deletion leads to osteopenia in mice through the inhibition of osteoblast terminal differentiation. J Bone Miner Res. 2013;28(11):2414-30. Epub 2013/05/02. doi: 10.1002/jbmr.1971. PubMed PMID: 23633228; PMCID: PMC3805719.
17. Chen L, Shi X, Weng SJ, Xie J, Tang JH, Yan DY, Wang BZ, Xie ZJ, Wu ZY, Yang L. Vitamin K2 Can Rescue the Dexamethasone-Induced Downregulation of Osteoblast Autophagy and Mitophagy Thereby Restoring Osteoblast Function In Vitro and In Vivo. Front Pharmacol. 2020;11:1209. Epub 2020/08/28. doi: 10.3389/fphar.2020.01209. PubMed PMID: 32848799; PMCID: PMC7431688.
18. Nollet M, Santucci-Darmanin S, Breuil V, Al-Sahlanee R, Cros C, Topi M, Momier D, Samson M, Pagnotta S, Cailleteau L, Battaglia S, Farlay D, Dacquin R, Barois N, Jurdic P, Boivin G, Heymann D, Lafont F, Lu SS, Dempster DW, Carle GF, Pierrefite-Carle V. Autophagy in osteoblasts is involved in mineralization and bone homeostasis. Autophagy. 2014;10(11):1965-77. Epub 2014/12/09. doi: 10.4161/auto.36182. PubMed PMID: 25484092; PMCID: PMC4502694.
19. Oliver L, Hue E, Priault M, Vallette FM. Basal autophagy decreased during the differentiation of human adult mesenchymal stem cells. Stem Cells Dev. 2012;21(15):2779-88. Epub 2012/04/24. doi: 10.1089/scd.2012.0124. PubMed PMID: 22519885.
20. Pierrefite-Carle V, Santucci-Darmanin S, Breuil V, Camuzard O, Carle GF. Autophagy in bone: Self-eating to stay in balance. Ageing Res Rev. 2015;24(Pt B):206-17. Epub 2015/09/01. doi: 10.1016/j.arr.2015.08.004. PubMed PMID: 26318060.
21. Damek-Poprawa M, Diemer T, Lopes VS, Lillo C, Harper DC, Marks MS, Wu Y, Sparrow JR, Rachel RA, Williams DS, Boesze-Battaglia K. Melanoregulin (MREG) modulates lysosome function in pigment epithelial cells. J Biol Chem. 2009;284(16):10877-89. Epub 2009/02/26. doi: 10.1074/jbc.M808857200. PubMed PMID: 19240024; PMCID: PMC2667774.
22. Frost LS, Lopes VS, Bragin A, Reyes-Reveles J, Brancato J, Cohen A, Mitchell CH, Williams DS, Boesze-Battaglia K. The Contribution of Melanoregulin to Microtubule-Associated Protein 1 Light Chain 3 (LC3) Associated Phagocytosis in Retinal Pigment Epithelium. Mol Neurobiol. 2015;52(3):1135-51. Epub 2014/10/11. doi: 10.1007/s12035-014-8920-5. PubMed PMID: 25301234; PMCID: PMC5531606.
23. Laha D, Deb M, Das H. KLF2 (kruppel-like factor 2 [lung]) regulates osteoclastogenesis by modulating autophagy. Autophagy. 2019;15(12):2063-75. Epub 2019/03/22. doi: 10.1080/15548627.2019.1596491. PubMed PMID: 30894058; PMCID: PMC6844519.
24. Wong SW, Huang BW, Hu X, Ho Kim E, Kolb JP, Padilla RJ, Xue P, Wang L, Oguin TH, 3rd, Miguez PA, Tseng HC, Ko CC, Martinez J. Global deletion of Optineurin results in altered type I IFN signaling and abnormal bone remodeling in a model of Paget's disease. Cell Death Differ. 2020;27(1):71-84. Epub 2019/05/12. doi: 10.1038/s41418-019-0341-6. PubMed PMID: 31076632; PMCID: PMC7205997.
25. Arai A, Kim S, Goldshteyn V, Kim T, Park NH, Wang CY, Kim RH. Beclin1 Modulates Bone Homeostasis by Regulating Osteoclast and Chondrocyte Differentiation. J Bone Miner Res. 2019;34(9):1753-66. Epub 2019/05/11. doi: 10.1002/jbmr.3756. PubMed PMID: 31074883; PMCID: PMC9346192.
26. DeSelm CJ, Miller BC, Zou W, Beatty WL, van Meel E, Takahata Y, Klumperman J, Tooze SA, Teitelbaum SL, Virgin HW. Autophagy proteins regulate the secretory component of

osteoclastic bone resorption. Dev Cell. 2011;21(5):966-74. Epub 2011/11/08. doi: 10.1016/j.devcel.2011.08.016. PubMed PMID: 22055344; PMCID: PMC3244473.
27. Chung YH, Yoon SY, Choi B, Sohn DH, Yoon KH, Kim WJ, Kim DH, Chang EJ. Microtubule-associated protein light chain 3 regulates Cdc42-dependent actin ring formation in osteoclast. Int J Biochem Cell Biol. 2012;44(6):989-97. Epub 2012/04/03. doi: 10.1016/j.biocel.2012.03.007. PubMed PMID: 22465708.
28. Sambandam Y, Townsend MT, Pierce JJ, Lipman CM, Haque A, Bateman TA, Reddy SV. Microgravity control of autophagy modulates osteoclastogenesis. Bone. 2014;61:125-31. Epub 2014/01/28. doi: 10.1016/j.bone.2014.01.004. PubMed PMID: 24463210; PMCID: PMC4384509.
29. O'Sullivan TN, Wu XS, Rachel RA, Huang JD, Swing DA, Matesic LE, Hammer JA, 3rd, Copeland NG, Jenkins NA. dsu functions in a MYO5A-independent pathway to suppress the coat color of dilute mice. Proc Natl Acad Sci U S A. 2004;101(48):16831-6. Epub 2004/11/20. doi: 10.1073/pnas.0407339101. PubMed PMID: 15550542; PMCID: PMC534743.
30. Gonçalves VP, Musskopf ML, Rivera-Concepcion A, Yu C, Wong SW, Tuin SA, Jiao Y, Susin C, Spolidorio LC, Miguez PA. Systemic Dietary Hesperidin Modulation of Osteoclastogenesis, Bone Homeostasis and Periodontal Disease in Mice. Int J Mol Sci. 2022;23(13). Epub 2022/07/10. doi: 10.3390/ijms23137100. PubMed PMID: 35806105; PMCID: PMC9266620.
31. Bouxsein ML, Boyd SK, Christiansen BA, Guldberg RE, Jepsen KJ, Müller R. Guidelines for assessment of bone microstructure in rodents using micro-computed tomography. J Bone Miner Res. 2010;25(7):1468-86. Epub 2010/06/10. doi: 10.1002/jbmr.141. PubMed PMID: 20533309.
32. Tevlin R, McArdle A, Chan CK, Pluvinage J, Walmsley GG, Wearda T, Marecic O, Hu MS, Paik KJ, Senarath-Yapa K, Atashroo DA, Zielins ER, Wan DC, Weissman IL, Longaker MT. Osteoclast derivation from mouse bone marrow. J Vis Exp. 2014(93):e52056. Epub 2014/11/20. doi: 10.3791/52056. PubMed PMID: 25407120; PMCID: PMC4353410.
33. Pal A, Al-Shaer AE, Guesdon W, Torres MJ, Armstrong M, Quinn K, Davis T, Reisdorph N, Neufer PD, Spangenburg EE, Carroll I, Bazinet RP, Halade GV, Clària J, Shaikh SR. Resolvin E1 derived from eicosapentaenoic acid prevents hyperinsulinemia and hyperglycemia in a host genetic manner. Faseb j. 2020;34(8):10640-56. Epub 2020/06/25. doi: 10.1096/fj.202000830R. PubMed PMID: 32579292; PMCID: PMC7497168.
34. Kiviranta R, Morko J, Alatalo SL, NicAmhlaoibh R, Risteli J, Laitala-Leinonen T, Vuorio E. Impaired bone resorption in cathepsin K-deficient mice is partially compensated for by enhanced osteoclastogenesis and increased expression of other proteases via an increased RANKL/OPG ratio. Bone. 2005;36(1):159-72. Epub 2005/01/25. doi: 10.1016/j.bone.2004.09.020. PubMed PMID: 15664014.
35. Boyle WJ, Simonet WS, Lacey DL. Osteoclast differentiation and activation. Nature. 2003;423(6937):337-42. Epub 2003/05/16. doi: 10.1038/nature01658. PubMed PMID: 12748652.
36. Scheller EL, Rosen CJ. What's the matter with MAT? Marrow adipose tissue, metabolism, and skeletal health. Ann N Y Acad Sci. 2014;1311(1):14-30. Epub 2014/03/22. doi: 10.1111/nyas.12327. PubMed PMID: 24650218; PMCID: PMC4049420.
37. Gao L, Liu G, Wu X, Liu C, Wang Y, Ma M, Ma Y, Hao Z. Osteocytes autophagy mediated by mTORC2 activation controls osteoblasts differentiation and osteoclasts activities under mechanical loading. Arch Biochem Biophys. 2023;742:109634. Epub 2023/05/11. doi: 10.1016/j.abb.2023.109634. PubMed PMID: 37164247.
38. Gavali S, Gupta MK, Daswani B, Wani MR, Sirdeshmukh R, Khatkhatay MI. Estrogen enhances human osteoblast survival and function via promotion of autophagy. Biochim Biophys Acta Mol Cell Res. 2019;1866(9):1498-507. Epub 2019/07/01. doi: 10.1016/j.bbamcr.2019.06.014. PubMed PMID: 31255720.
39. Meng X, Dong Y, Yu X, Wang D, Wang S, Chen S, Pang S. MREG suppresses thyroid cancer cell invasion and proliferation by inhibiting Akt-mTOR signaling. Biochem Biophys Res Commun. 2017;491(1):72-8. Epub 2017/07/13. doi: 10.1016/j.bbrc.2017.07.044. PubMed PMID: 28698135.

40. Ejaz A, Mitterberger MC, Lu Z, Mattesich M, Zwierzina ME, Hörl S, Kaiser A, Viertler HP, Rostek U, Meryk A, Khalid S, Pierer G, Bast RC, Jr., Zwerschke W. Weight Loss Upregulates the Small GTPase DIRAS3 in Human White Adipose Progenitor Cells, Which Negatively Regulates Adipogenesis and Activates Autophagy via Akt-mTOR Inhibition. EBioMedicine. 2016;6:149-61. Epub 2016/05/24. doi: 10.1016/j.ebiom.2016.03.030. PubMed PMID: 27211557; PMCID: PMC4856797.
41. Song BQ, Chi Y, Li X, Du WJ, Han ZB, Tian JJ, Li JJ, Chen F, Wu HH, Han LX, Lu SH, Zheng YZ, Han ZC. Inhibition of Notch Signaling Promotes the Adipogenic Differentiation of Mesenchymal Stem Cells Through Autophagy Activation and PTEN-PI3K/AKT/mTOR Pathway. Cell Physiol Biochem. 2015;36(5):1991-2002. Epub 2015/07/24. doi: 10.1159/000430167. PubMed PMID: 26202359.
42. Wang S, Wang J, Wang S, Tao R, Yi J, Chen M, Zhao Z. mTOR Signaling Pathway in Bone Diseases Associated with Hyperglycemia. Int J Mol Sci. 2023;24(11). Epub 2023/06/10. doi: 10.3390/ijms24119198. PubMed PMID: 37298150; PMCID: PMC10252649.
43. Blasi I, Korostoff J, Dhingra A, Reyes-Reveles J, Shenker BJ, Shahabuddin N, Alexander D, Lally ET, Bragin A, Boesze-Battaglia K. Variants of Porphyromonas gingivalis lipopolysaccharide alter lipidation of autophagic protein, microtubule-associated protein 1 light chain 3, LC3. Mol Oral Microbiol. 2016;31(6):486-500. Epub 2016/11/05. doi: 10.1111/omi.12141. PubMed PMID: 26452236.
44. Glatt V, Canalis E, Stadmeyer L, Bouxsein ML. Age-related changes in trabecular architecture differ in female and male C57BL/6J mice. J Bone Miner Res. 2007;22(8):1197-207. Epub 2007/05/10. doi: 10.1359/jbmr.070507. PubMed PMID: 17488199.
45. Chen J, Tu X, Esen E, Joeng KS, Lin C, Arbeit JM, Rüegg MA, Hall MN, Ma L, Long F. WNT7B promotes bone formation in part through mTORC1. PLoS Genet. 2014;10(1):e1004145. Epub 2014/02/06. doi: 10.1371/journal.pgen.1004145. PubMed PMID: 24497849; PMCID: PMC3907335.
46. Klionsky DJ, Abdalla FC, Abeliovich H, Abraham RT, Acevedo-Arozena A, Adeli K, Agholme L, Agnello M, Agostinis P, Aguirre-Ghiso JA, Ahn HJ, Ait-Mohamed O, Ait-Si-Ali S, Akematsu T, Akira S, Al-Younes HM, Al-Zeer MA, Albert ML, Albin RL, Alegre-Abarrategui J, Aleo MF, Alirezaei M, Almasan A, Almonte-Becerril M, Amano A, Amaravadi R, Amarnath S, Amer AO, Andrieu-Abadie N, Anantharam V, Ann DK, Anoopkumar-Dukie S, Aoki H, Apostolova N, Arancia G, Aris JP, Asanuma K, Asare NY, Ashida H, Askanas V, Askew DS, Auberger P, Baba M, Backues SK, Baehrecke EH, Bahr BA, Bai XY, Bailly Y, Baiocchi R, Baldini G, Balduini W, Ballabio A, Bamber BA, Bampton ET, Bánhegyi G, Bartholomew CR, Bassham DC, Bast RC, Jr., Batoko H, Bay BH, Beau I, Béchet DM, Begley TJ, Behl C, Behrends C, Bekri S, Bellaire B, Bendall LJ, Benetti L, Berliocchi L, Bernardi H, Bernassola F, Besteiro S, Bhatia-Kissova I, Bi X, Biard-Piechaczyk M, Blum JS, Boise LH, Bonaldo P, Boone DL, Bornhauser BC, Bortoluci KR, Bossis I, Bost F, Bourquin JP, Boya P, Boyer-Guittaut M, Bozhkov PV, Brady NR, Brancolini C, Brech A, Brenman JE, Brennand A, Bresnick EH, Brest P, Bridges D, Bristol ML, Brookes PS, Brown EJ, Brumell JH, Brunetti-Pierri N, Brunk UT, Bulman DE, Bultman SJ, Bultynck G, Burbulla LF, Bursch W, Butchar JP, Buzgariu W, Bydlowski SP, Cadwell K, Cahová M, Cai D, Cai J, Cai Q, Calabretta B, Calvo-Garrido J, Camougrand N, Campanella M, Campos-Salinas J, Candi E, Cao L, Caplan AB, Carding SR, Cardoso SM, Carew JS, Carlin CR, Carmignac V, Carneiro LA, Carra S, Caruso RA, Casari G, Casas C, Castino R, Cebollero E, Cecconi F, Celli J, Chaachouay H, Chae HJ, Chai CY, Chan DC, Chan EY, Chang RC, Che CM, Chen CC, Chen GC, Chen GQ, Chen M, Chen Q, Chen SS, Chen W, Chen X, Chen X, Chen X, Chen YG, Chen Y, Chen Y, Chen YJ, Chen Z, Cheng A, Cheng CH, Cheng Y, Cheong H, Cheong JH, Cherry S, Chess-Williams R, Cheung ZH, Chevet E, Chiang HL, Chiarelli R, Chiba T, Chin LS, Chiou SH, Chisari FV, Cho CH, Cho DH, Choi AM, Choi D, Choi KS, Choi ME, Chouaib S, Choubey D, Choubey V, Chu CT, Chuang TH, Chueh SH, Chun T, Chwae YJ, Chye ML, Ciarcia R, Ciriolo MR, Clague MJ, Clark RS, Clarke PG, Clarke R, Codogno P, Coller HA, Colombo MI, Comincini S, Condello M, Condorelli F, Cookson MR, Coombs GH, Coppens I, Corbalan R, Cossart P,

Costelli P, Costes S, Coto-Montes A, Couve E, Coxon FP, Cregg JM, Crespo JL, Cronjé MJ, Cuervo AM, Cullen JJ, Czaja MJ, D'Amelio M, Darfeuille-Michaud A, Davids LM, Davies FE, De Felici M, de Groot JF, de Haan CA, De Martino L, De Milito A, De Tata V, Debnath J, Degterev A, Dehay B, Delbridge LM, Demarchi F, Deng YZ, Dengjel J, Dent P, Denton D, Deretic V, Desai SD, Devenish RJ, Di Gioacchino M, Di Paolo G, Di Pietro C, Díaz-Araya G, Díaz-Laviada I, Diaz-Meco MT, Diaz-Nido J, Dikic I, Dinesh-Kumar SP, Ding WX, Distelhorst CW, Diwan A, Djavaheri-Mergny M, Dokudovskaya S, Dong Z, Dorsey FC, Dosenko V, Dowling JJ, Doxsey S, Dreux M, Drew ME, Duan Q, Duchosal MA, Duff K, Dugail I, Durbeej M, Duszenko M, Edelstein CL, Edinger AL, Egea G, Eichinger L, Eissa NT, Ekmekcioglu S, El-Deiry WS, Elazar Z, Elgendy M, Ellerby LM, Eng KE, Engelbrecht AM, Engelender S, Erenpreisa J, Escalante R, Esclatine A, Eskelinen EL, Espert L, Espina V, Fan H, Fan J, Fan QW, Fan Z, Fang S, Fang Y, Fanto M, Fanzani A, Farkas T, Farré JC, Faure M, Fechheimer M, Feng CG, Feng J, Feng Q, Feng Y, Fésüs L, Feuer R, Figueiredo-Pereira ME, Fimia GM, Fingar DC, Finkbeiner S, Finkel T, Finley KD, Fiorito F, Fisher EA, Fisher PB, Flajolet M, Florez-McClure ML, Florio S, Fon EA, Fornai F, Fortunato F, Fotedar R, Fowler DH, Fox HS, Franco R, Frankel LB, Fransen M, Fuentes JM, Fueyo J, Fujii J, Fujisaki K, Fujita E, Fukuda M, Furukawa RH, Gaestel M, Gailly P, Gajewska M, Galliot B, Galy V, Ganesh S, Ganetzky B, Ganley IG, Gao FB, Gao GF, Gao J, Garcia L, Garcia-Manero G, Garcia-Marcos M, Garmyn M, Gartel AL, Gatti E, Gautel M, Gawriluk TR, Gegg ME, Geng J, Germain M, Gestwicki JE, Gewirtz DA, Ghavami S, Ghosh P, Giammarioli AM, Giatromanolaki AN, Gibson SB, Gilkerson RW, Ginger ML, Ginsberg HN, Golab J, Goligorsky MS, Golstein P, Gomez-Manzano C, Goncu E, Gongora C, Gonzalez CD, Gonzalez R, González-Estévez C, González-Polo RA, Gonzalez-Rey E, Gorbunov NV, Gorski S, Goruppi S, Gottlieb RA, Gozuacik D, Granato GE, Grant GD, Green KN, Gregorc A, Gros F, Grose C, Grunt TW, Gual P, Guan JL, Guan KL, Guichard SM, Gukovskaya AS, Gukovsky I, Gunst J, Gustafsson AB, Halayko AJ, Hale AN, Halonen SK, Hamasaki M, Han F, Han T, Hancock MK, Hansen M, Harada H, Harada M, Hardt SE, Harper JW, Harris AL, Harris J, Harris SD, Hashimoto M, Haspel JA, Hayashi S, Hazelhurst LA, He C, He YW, Hébert MJ, Heidenreich KA, Helfrich MH, Helgason GV, Henske EP, Herman B, Herman PK, Hetz C, Hilfiker S, Hill JA, Hocking LJ, Hofman P, Hofmann TG, Höhfeld J, Holyoake TL, Hong MH, Hood DA, Hotamisligil GS, Houwerzijl EJ, Høyer-Hansen M, Hu B, Hu CA, Hu HM, Hua Y, Huang C, Huang J, Huang S, Huang WP, Huber TB, Huh WK, Hung TH, Hupp TR, Hur GM, Hurley JB, Hussain SN, Hussey PJ, Hwang JJ, Hwang S, Ichihara A, Ilkhanizadeh S, Inoki K, Into T, Iovane V, Iovanna JL, Ip NY, Isaka Y, Ishida H, Isidoro C, Isobe K, Iwasaki A, Izquierdo M, Izumi Y, Jaakkola PM, Jäättelä M, Jackson GR, Jackson WT, Janji B, Jendrach M, Jeon JH, Jeung EB, Jiang H, Jiang H, Jiang JX, Jiang M, Jiang Q, Jiang X, Jiang X, Jiménez A, Jin M, Jin S, Joe CO, Johansen T, Johnson DE, Johnson GV, Jones NL, Joseph B, Joseph SK, Joubert AM, Juhász G, Juillerat-Jeanneret L, Jung CH, Jung YK, Kaarniranta K, Kaasik A, Kabuta T, Kadowaki M, Kagedal K, Kamada Y, Kaminskyy VO, Kampinga HH, Kanamori H, Kang C, Kang KB, Kang KI, Kang R, Kang YA, Kanki T, Kanneganti TD, Kanno H, Kanthasamy AG, Kanthasamy A, Karantza V, Kaushal GP, Kaushik S, Kawazoe Y, Ke PY, Kehrl JH, Kelekar A, Kerkhoff C, Kessel DH, Khalil H, Kiel JA, Kiger AA, Kihara A, Kim DR, Kim DH, Kim DH, Kim EK, Kim HR, Kim JS, Kim JH, Kim JC, Kim JK, Kim PK, Kim SW, Kim YS, Kim Y, Kimchi A, Kimmelman AC, King JS, Kinsella TJ, Kirkin V, Kirshenbaum LA, Kitamoto K, Kitazato K, Klein L, Klimecki WT, Klucken J, Knecht E, Ko BC, Koch JC, Koga H, Koh JY, Koh YH, Koike M, Komatsu M, Kominami E, Kong HJ, Kong WJ, Korolchuk VI, Kotake Y, Koukourakis MI, Kouri Flores JB, Kovács AL, Kraft C, Krainc D, Krämer H, Kretz-Remy C, Krichevsky AM, Kroemer G, Krüger R, Krut O, Ktistakis NT, Kuan CY, Kucharczyk R, Kumar A, Kumar R, Kumar S, Kundu M, Kung HJ, Kurz T, Kwon HJ, La Spada AR, Lafont F, Lamark T, Landry J, Lane JD, Lapaquette P, Laporte JF, László L, Lavandero S, Lavoie JN, Layfield R, Lazo PA, Le W, Le Cam L, Ledbetter DJ, Lee AJ, Lee BW, Lee GM, Lee J, Lee JH, Lee M, Lee MS, Lee SH, Leeuwenburgh C, Legembre P, Legouis R, Lehmann M, Lei HY, Lei QY, Leib DA, Leiro J, Lemasters JJ, Lemoine A, Lesniak MS, Lev D, Levenson VV, Levine B, Levy E, Li F, Li JL, Li L, Li S, Li W, Li XJ, Li YB, Li YP, Liang C, Liang Q, Liao YF, Liberski PP, Lieberman A, Lim HJ,

Lim KL, Lim K, Lin CF, Lin FC, Lin J, Lin JD, Lin K, Lin WW, Lin WC, Lin YL, Linden R, Lingor P, Lippincott-Schwartz J, Lisanti MP, Liton PB, Liu B, Liu CF, Liu K, Liu L, Liu QA, Liu W, Liu YC, Liu Y, Lockshin RA, Lok CN, Lonial S, Loos B, Lopez-Berestein G, López-Otín C, Lossi L, Lotze MT, Lőw P, Lu B, Lu B, Lu B, Lu Z, Luciano F, Lukacs NW, Lund AH, Lynch-Day MA, Ma Y, Macian F, MacKeigan JP, Macleod KF, Madeo F, Maiuri L, Maiuri MC, Malagoli D, Malicdan MC, Malorni W, Man N, Mandelkow EM, Manon S, Manov I, Mao K, Mao X, Mao Z, Marambaud P, Marazziti D, Marcel YL, Marchbank K, Marchetti P, Marciniak SJ, Marcondes M, Mardi M, Marfe G, Mariño G, Markaki M, Marten MR, Martin SJ, Martinand-Mari C, Martinet W, Martinez-Vicente M, Masini M, Matarrese P, Matsuo S, Matteoni R, Mayer A, Mazure NM, McConkey DJ, McConnell MJ, McDermott C, McDonald C, McInerney GM, McKenna SL, McLaughlin B, McLean PJ, McMaster CR, McQuibban GA, Meijer AJ, Meisler MH, Meléndez A, Melia TJ, Melino G, Mena MA, Menendez JA, Menna-Barreto RF, Menon MB, Menzies FM, Mercer CA, Merighi A, Merry DE, Meschini S, Meyer CG, Meyer TF, Miao CY, Miao JY, Michels PA, Michiels C, Mijaljica D, Milojkovic A, Minucci S, Miracco C, Miranti CK, Mitroulis I, Miyazawa K, Mizushima N, Mograbi B, Mohseni S, Molero X, Mollereau B, Mollinedo F, Momoi T, Monastyrska I, Monick MM, Monteiro MJ, Moore MN, Mora R, Moreau K, Moreira PI, Moriyasu Y, Moscat J, Mostowy S, Mottram JC, Motyl T, Moussa CE, Müller S, Muller S, Münger K, Münz C, Murphy LO, Murphy ME, Musarò A, Mysorekar I, Nagata E, Nagata K, Nahimana A, Nair U, Nakagawa T, Nakahira K, Nakano H, Nakatogawa H, Nanjundan M, Naqvi NI, Narendra DP, Narita M, Navarro M, Nawrocki ST, Nazarko TY, Nemchenko A, Netea MG, Neufeld TP, Ney PA, Nezis IP, Nguyen HP, Nie D, Nishino I, Nislow C, Nixon RA, Noda T, Noegel AA, Nogalska A, Noguchi S, Notterpek L, Novak I, Nozaki T, Nukina N, Nürnberger T, Nyfeler B, Obara K, Oberley TD, Oddo S, Ogawa M, Ohashi T, Okamoto K, Oleinick NL, Oliver FJ, Olsen LJ, Olsson S, Opota O, Osborne TF, Ostrander GK, Otsu K, Ou JH, Ouimet M, Overholtzer M, Ozpolat B, Paganetti P, Pagnini U, Pallet N, Palmer GE, Palumbo C, Pan T, Panaretakis T, Pandey UB, Papackova Z, Papassideri I, Paris I, Park J, Park OK, Parys JB, Parzych KR, Patschan S, Patterson C, Pattingre S, Pawelek JM, Peng J, Perlmutter DH, Perrotta I, Perry G, Pervaiz S, Peter M, Peters GJ, Petersen M, Petrovski G, Phang JM, Piacentini M, Pierre P, Pierrefite-Carle V, Pierron G, Pinkas-Kramarski R, Piras A, Piri N, Platanias LC, Pöggeler S, Poirot M, Poletti A, Poüs C, Pozuelo-Rubio M, Prætorius-Ibba M, Prasad A, Prescott M, Priault M, Produit-Zengaffinen N, Progulske-Fox A, Proikas-Cezanne T, Przedborski S, Przyklenk K, Puertollano R, Puyal J, Qian SB, Qin L, Qin ZH, Quaggin SE, Raben N, Rabinowich H, Rabkin SW, Rahman I, Rami A, Ramm G, Randall G, Randow F, Rao VA, Rathmell JC, Ravikumar B, Ray SK, Reed BH, Reed JC, Reggiori F, Régnier-Vigouroux A, Reichert AS, Reiners JJ, Jr., Reiter RJ, Ren J, Revuelta JL, Rhodes CJ, Ritis K, Rizzo E, Robbins J, Roberge M, Roca H, Roccheri MC, Rocchi S, Rodemann HP, Rodríguez de Córdoba S, Rohrer B, Roninson IB, Rosen K, Rost-Roszkowska MM, Rouis M, Rouschop KM, Rovetta F, Rubin BP, Rubinsztein DC, Ruckdeschel K, Rucker EB, 3rd, Rudich A, Rudolf E, Ruiz-Opazo N, Russo R, Rusten TE, Ryan KM, Ryter SW, Sabatini DM, Sadoshima J, Saha T, Saitoh T, Sakagami H, Sakai Y, Salekdeh GH, Salomoni P, Salvaterra PM, Salvesen G, Salvioli R, Sanchez AM, Sánchez-Alcázar JA, Sánchez-Prieto R, Sandri M, Sankar U, Sansanwal P, Santambrogio L, Saran S, Sarkar S, Sarwal M, Sasakawa C, Sasnauskiene A, Sass M, Sato K, Sato M, Schapira AH, Scharl M, Schätzl HM, Scheper W, Schiaffino S, Schneider C, Schneider ME, Schneider-Stock R, Schoenlein PV, Schorderet DF, Schüller C, Schwartz GK, Scorrano L, Sealy L, Seglen PO, Segura-Aguilar J, Seiliez I, Seleverstov O, Sell C, Seo JB, Separovic D, Setaluri V, Setoguchi T, Settembre C, Shacka JJ, Shanmugam M, Shapiro IM, Shaulian E, Shaw RJ, Shelhamer JH, Shen HM, Shen WC, Sheng ZH, Shi Y, Shibuya K, Shidoji Y, Shieh JJ, Shih CM, Shimada Y, Shimizu S, Shintani T, Shirihai OS, Shore GC, Sibirny AA, Sidhu SB, Sikorska B, Silva-Zacarin EC, Simmons A, Simon AK, Simon HU, Simone C, Simonsen A, Sinclair DA, Singh R, Sinha D, Sinicrope FA, Sirko A, Siu PM, Sivridis E, Skop V, Skulachev VP, Slack RS, Smaili SS, Smith DR, Soengas MS, Soldati T, Song X, Sood AK, Soong TW, Sotgia F, Spector SA, Spies CD, Springer W, Srinivasula SM, Stefanis L, Steffan JS, Stendel R, Stenmark H, Stephanou A, Stern ST, Sternberg C, Stork B, Strålfors P, Subauste CS, Sui X, Sulzer D, Sun J, Sun SY, Sun ZJ, Sung

JJ, Suzuki K, Suzuki T, Swanson MS, Swanton C, Sweeney ST, Sy LK, Szabadkai G, Tabas I, Taegtmeyer H, Tafani M, Takács-Vellai K, Takano Y, Takegawa K, Takemura G, Takeshita F, Talbot NJ, Tan KS, Tanaka K, Tanaka K, Tang D, Tang D, Tanida I, Tannous BA, Tavernarakis N, Taylor GS, Taylor GA, Taylor JP, Terada LS, Terman A, Tettamanti G, Thevissen K, Thompson CB, Thorburn A, Thumm M, Tian F, Tian Y, Tocchini-Valentini G, Tolkovsky AM, Tomino Y, Tönges L, Tooze SA, Tournier C, Tower J, Towns R, Trajkovic V, Travassos LH, Tsai TF, Tschan MP, Tsubata T, Tsung A, Turk B, Turner LS, Tyagi SC, Uchiyama Y, Ueno T, Umekawa M, Umemiya-Shirafuji R, Unni VK, Vaccaro MI, Valente EM, Van den Berghe G, van der Klei IJ, van Doorn W, van Dyk LF, van Egmond M, van Grunsven LA, Vandenabeele P, Vandenberghe WP, Vanhorebeek I, Vaquero EC, Velasco G, Vellai T, Vicencio JM, Vierstra RD, Vila M, Vindis C, Viola G, Viscomi MT, Voitsekhovskaja OV, von Haefen C, Votruba M, Wada K, Wade-Martins R, Walker CL, Walsh CM, Walter J, Wan XB, Wang A, Wang C, Wang D, Wang F, Wang F, Wang G, Wang H, Wang HG, Wang HD, Wang J, Wang K, Wang M, Wang RC, Wang X, Wang X, Wang YJ, Wang Y, Wang Z, Wang ZC, Wang Z, Wansink DG, Ward DM, Watada H, Waters SL, Webster P, Wei L, Weihl CC, Weiss WA, Welford SM, Wen LP, Whitehouse CA, Whitton JL, Whitworth AJ, Wileman T, Wiley JW, Wilkinson S, Willbold D, Williams RL, Williamson PR, Wouters BG, Wu C, Wu DC, Wu WK, Wyttenbach A, Xavier RJ, Xi Z, Xia P, Xiao G, Xie Z, Xie Z, Xu DZ, Xu J, Xu L, Xu X, Yamamoto A, Yamamoto A, Yamashina S, Yamashita M, Yan X, Yanagida M, Yang DS, Yang E, Yang JM, Yang SY, Yang W, Yang WY, Yang Z, Yao MC, Yao TP, Yeganeh B, Yen WL, Yin JJ, Yin XM, Yoo OJ, Yoon G, Yoon SY, Yorimitsu T, Yoshikawa Y, Yoshimori T, Yoshimoto K, You HJ, Youle RJ, Younes A, Yu L, Yu L, Yu SW, Yu WH, Yuan ZM, Yue Z, Yun CH, Yuzaki M, Zabirnyk O, Silva-Zacarin E, Zacks D, Zacksenhaus E, Zaffaroni N, Zakeri Z, Zeh HJ, 3rd, Zeitlin SO, Zhang H, Zhang HL, Zhang J, Zhang JP, Zhang L, Zhang L, Zhang MY, Zhang XD, Zhao M, Zhao YF, Zhao Y, Zhao ZJ, Zheng X, Zhivotovsky B, Zhong Q, Zhou CZ, Zhu C, Zhu WG, Zhu XF, Zhu X, Zhu Y, Zoladek T, Zong WX, Zorzano A, Zschocke J, Zuckerbraun B. Guidelines for the use and interpretation of assays for monitoring autophagy. Autophagy. 2012;8(4):445-544. Epub 2012/09/12. doi: 10.4161/auto.19496. PubMed PMID: 22966490; PMCID: PMC3404883.

47. Cao JJ, Wronski TJ, Iwaniec U, Phleger L, Kurimoto P, Boudignon B, Halloran BP. Aging increases stromal/osteoblastic cell-induced osteoclastogenesis and alters the osteoclast precursor pool in the mouse. J Bone Miner Res. 2005;20(9):1659-68. Epub 2005/08/02. doi: 10.1359/jbmr.050503. PubMed PMID: 16059637.

48. Kim KH, Lee MS. Autophagy as a crosstalk mediator of metabolic organs in regulation of energy metabolism. Rev Endocr Metab Disord. 2014;15(1):11-20. Epub 2013/10/03. doi: 10.1007/s11154-013-9272-6. PubMed PMID: 24085381.

49. Singh R, Cuervo AM. Autophagy in the cellular energetic balance. Cell Metab. 2011;13(5):495-504. Epub 2011/05/03. doi: 10.1016/j.cmet.2011.04.004. PubMed PMID: 21531332; PMCID: PMC3099265.

Fig 1. Melanoregulin (MREG) mutation and bone homeostasis at 4 months (A, B) and 10 months (C, D). Trabecular bone and bone volume assessed via microcomputed tomography (mCT) show significant changes, $p<0.05$, at 10 months of age (C, D). * indicates statistical difference compared to wild-type (WT). At 10 months, cortical parameters were not statistically different (E). 3D rendering of trabecular bone shows clear evidence of improved trabecular fill in MREG knock out (KO) mice at 10 months of age (lower panel). n= 4-5 male mice.

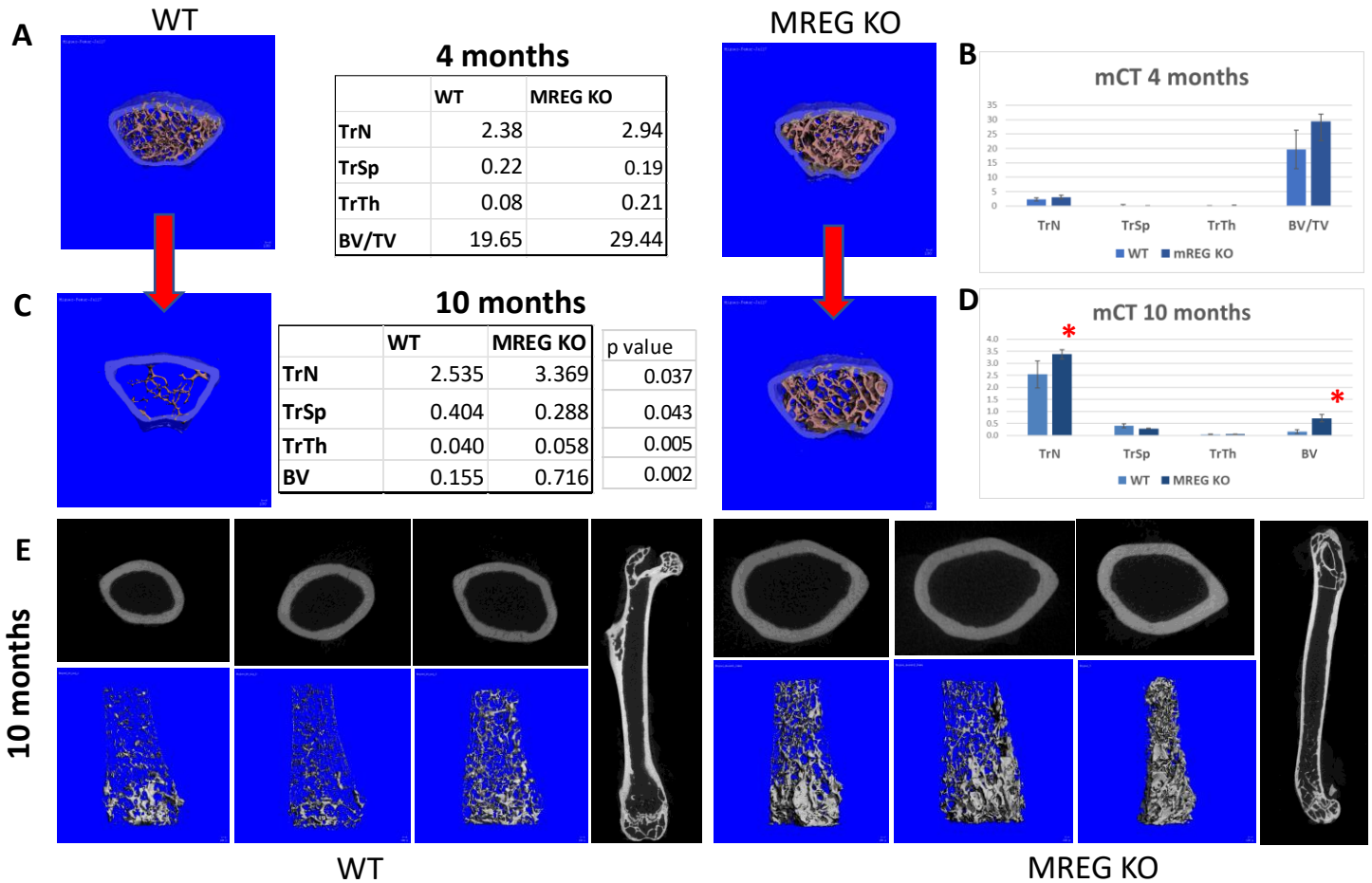

4 months

	WT	MREG KO
TrN	2.38	2.94
TrSp	0.22	0.19
TrTh	0.08	0.21
BV/TV	19.65	29.44

10 months

	WT	MREG KO	p value
TrN	2.535	3.369	0.037
TrSp	0.404	0.288	0.043
TrTh	0.040	0.058	0.005
BV	0.155	0.716	0.002

Fig 2. Mouse femurs of MREG mutant mice at 4 months have similar gross morphometric characteristics within the growth plate (A). At 10 months of age, MREG mice showed clear differences in cell composition. Adipocytes are present only in WT mice (red arrow) (B), suggesting a cell fate effect by MREG absence.

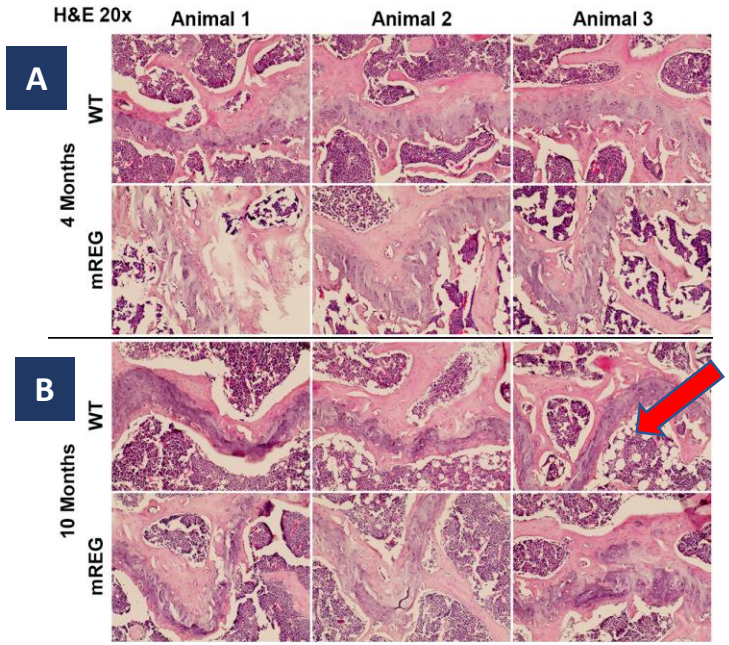

Fig 3. Osteoclast activity was assessed by TRAP staining in 4 and 10-month-old mice femurs (n=4-5). At 4 months, the osteoclast count was not different in WT vs. MREG mutant mice (A, B). At 10 months, differences were observed in the TRAP-stained cells for MREG mice (C, D). There was a significant increase in osteoclast numbers per total area in MREG mice at 10 months (E, * indicate statistical difference at $p < 0.05$).

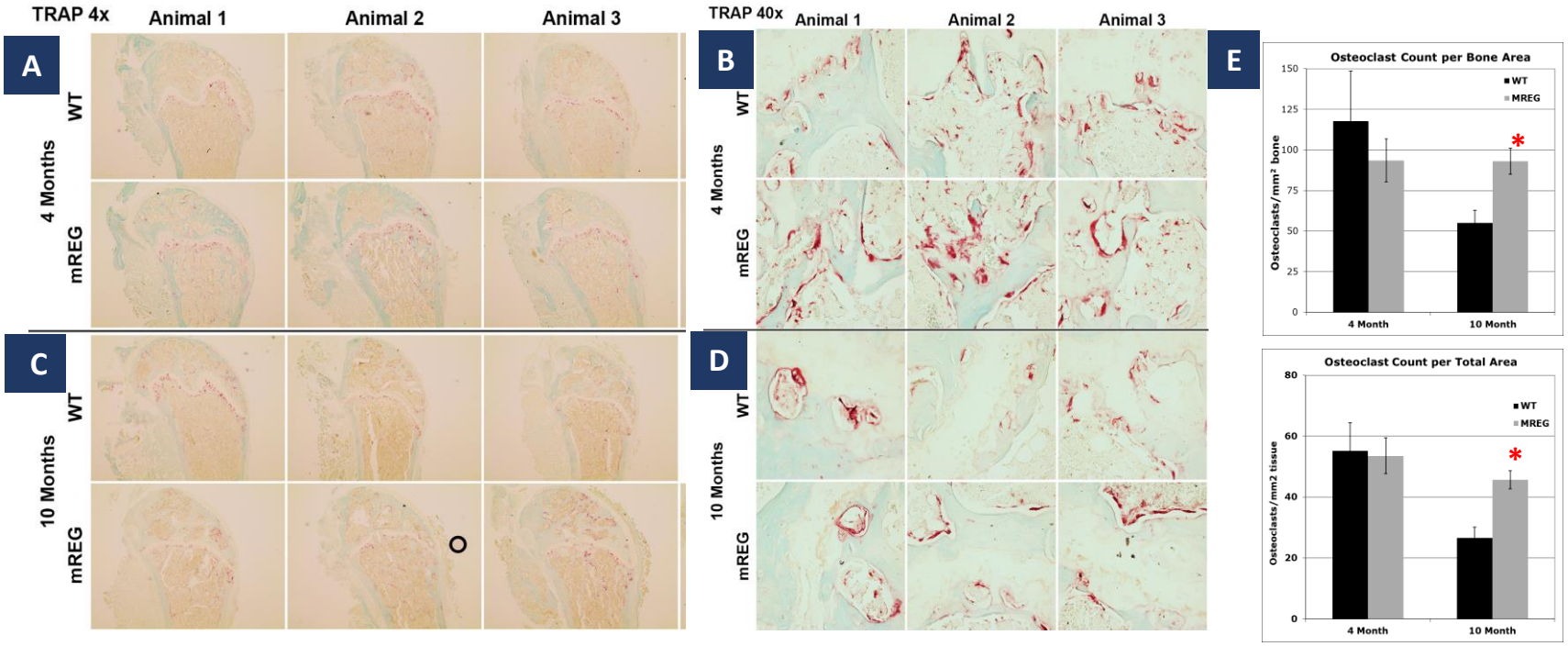

Fig 4. Bone marrow-derived osteoclasts from WT and MREG mutant (-/-) mice differentiate ex vivo similarly, as shown by TRAP staining (A) and Western Blot for osteoclastogenesis master marker Nfatc1 (B). Bone resorptive capacity is altered in MREG mutant (-/-) mice (C) with statistically significant differences in resorption pits generated by MREG mutatnt-derived osteoclasts (D) ($p<0.05$). Quantification of the resorptive area was statistically lower in MREG mutant mice.

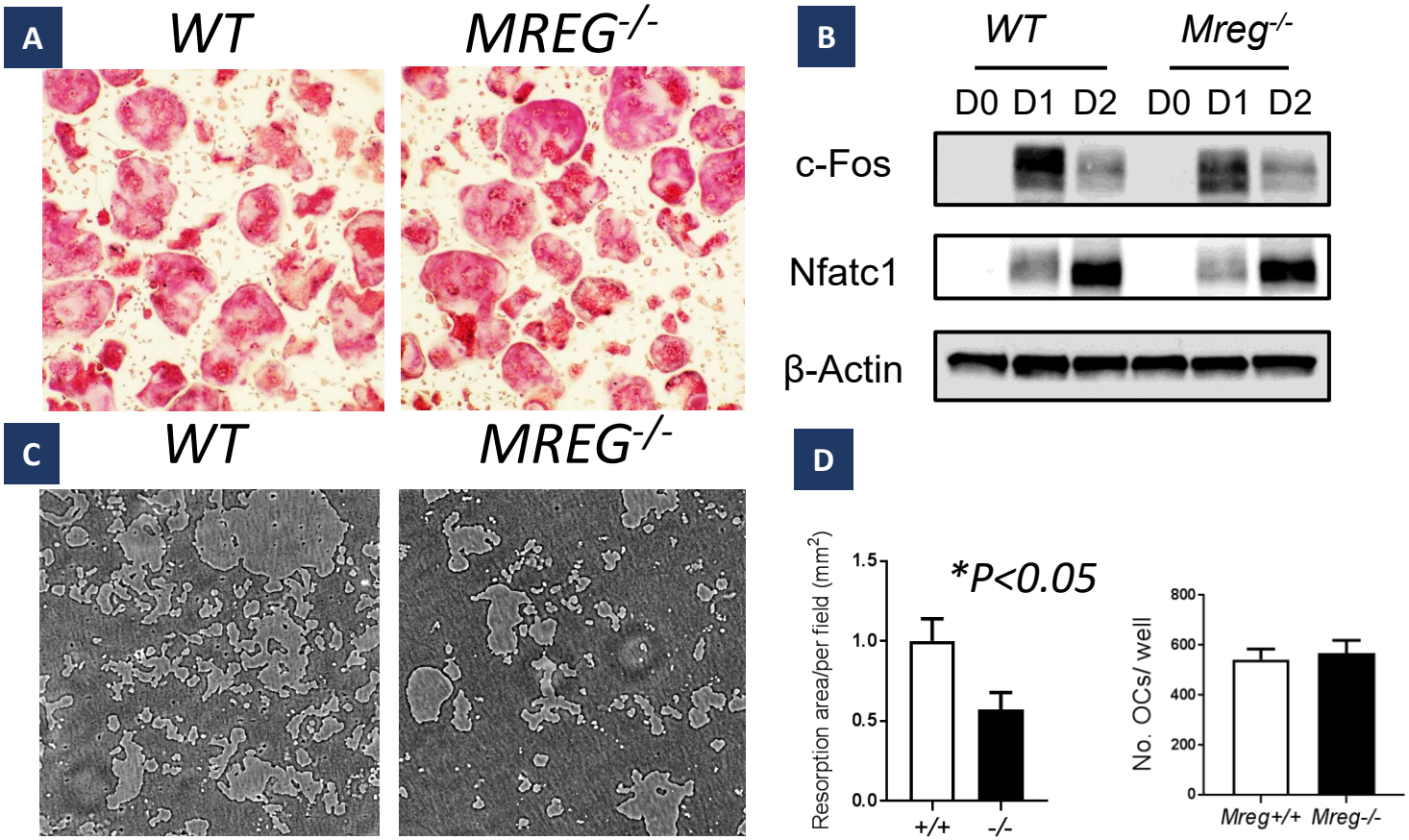

Fig 5. Quantitative analysis of lean and fat content of WT and MREG knock out (KO) mutant mice at 10 months of age via EchoMRI. Lean mass was significantly higher in MREG mutant male mice compared to WT at 10 months of age (A in red, B). WT mice at 4 months were not evaluated (not observed = no obs).

A

EchoMRI	Lean		Fat		Weight	
	Male		Male		Male	
	4 months	10 months	4 months	10 months	4 months	10 months
MREG KO	26.15(±3.58)	28.09(±0.92)	1.89(±0.75)	8.66(±5.56)	30.13(±4.38)	39.00(±6.15)
WT	no obs	25.02(±1.47)	no obs	9.02(±2.59)	no obs	36.28(±4.20)
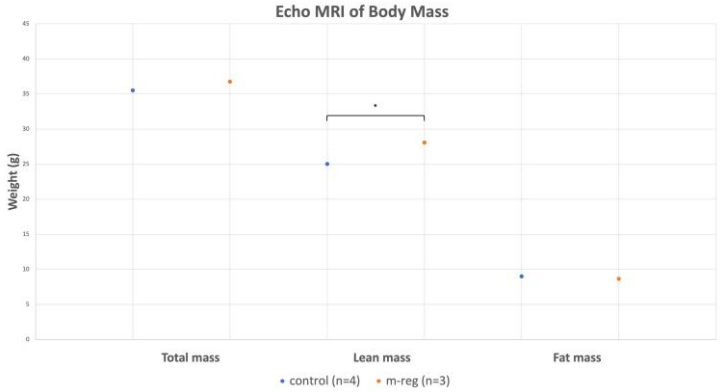
B